JOURNAL OF MATERIALS SCIENCE 15 (1980) 3141–3149

On the formation of thermally sprayed alumina coatings

R. McPHERSON*
Laboratoire de Thermodynamique, Université de Limoges, Limoges, France

A model for the fomation of thermally sprayed alumina coatings is proposed. The spreading and crystallization of liquid droplets on impact with the substrate are analysed and the thermal history of individual particles related to the kinetics of nucleation of γ-Al_2O_3 to other forms. The results suggest that under the usual spraying conditions undercooling of the liquid droplets is such that γ-Al_2O_3 nucleates in preference to α-Al_2O_3 and the cooling rate after solidification is sufficiently rapid to prevent transformation to δ-Al_2O_3 or α-Al_2O_3. Transformation of initially formed γ-Al_2O_3 to α-Al_2O_3 appears to be possible only if the lamellae formed on impact are thicker than about 10 μm if the substrate is heated to about 1000° C, or if the thickness is greater than about 20 μm on an unheated substrate. The α-Al_2O_3 generally observed in thermally sprayed coatings is the result of crystallization from pre-existing nuclei arising from incomplete melting of the feed material.

1. Introduction

Ceramic coatings, prepared by the projection of a stream of molten particles at high velocity against the material to be coated, are widely used to provide wear, thermal or corrosion protection. The droplet spray may be produced either by passing suitable powders or a rod through a combustion flame (flame-spraying) or by the injection of powder into a direct current plasma jet (plasma-spraying). The two processes are identical in principle, however, the higher temperatures and gas velocities in plasma jets result in a higher velocity molten particle spray with no practical limitations on the materials sprayed imposed because of melting point. The inert nature of the plasma gases is also an advantage in certain circumstances. The microstructure of both flame- and plasma-sprayed coatings consists of a series of overlapping lamellae produced by the spread and rapid solidification of the impinging droplets. Under favourable conditions porosities of less than 10% may be achieved with good adhesion to the substrate [1].

Early workers made the interesting observation that flame-sprayed alumina coatings consisted, not of the expected equilibrium α-form, but predominantly of the metastable γ-Al_2O_3 structure which, up to that time, had generally been regarded as a "low temperature" form observed as a product of calcination of hydroxides and salts, and of the oxidation of aluminium [2]. Since the physical properties of γ-Al_2O_3 are generally inferior to those of α-Al_2O_3, there has been some interest in the factors controlling the crystalline structure of alumina deposits. This has been the case particularly with attempts to produce alumina shapes by spraying onto a removable core. Since γ-Al_2O_3 transforms to α-Al_2O_3 on heating to above approximately 1100° C it is possible to convert sprayed deposits completely to α-Al_2O_3 by heat treatment, although the lower density of γ-Al_2O_3 ($3.6\,g\,cm^{-3}$ compared with $4.0\,g\,cm^{-3}$ for α-Al_2O_3) results in an increase in porosity during this transformation [2–4].

Under most conditions flame- and plasma-sprayed coatings contain some α-Al_2O_3 in addition to γ-Al_2O_3 [3, 5, 6]. It has been reported that the proportion of α-Al_2O_3 in flame-sprayed coatings increases linearly with substrate temperature reaching 85%, by weight, at 800° C [7]. No

*Permanent address: Department of Materials Engineering, Monash University, Clayton, Victoria 3168, Australia.

0022–2461/80/123141–09$02.90/0

significant increase in the α-Al_2O_3 content of plasma-sprayed Al_2O_3 was observed at substrate temperatures up to 900° C [5]. Coatings consisting completely of α-Al_2O_3 may be produced by spraying onto a substrate heated above the transformation temperature of about 1100° C [5], but in order to achieve low porosity the substrate must be heated to approximately 1450° C [8].

Sprayed coatings have also been reported to contain other metastable forms of alumina, notably δ-Al_2O_3 and θ-Al_2O_3. Heating of γ-Al_2O_3 results in the formation of δ-Al_2O_3 and θ-Al_2O_3 as intermediate phases in transformation to α-Al_2O_3 so that their formation when spraying onto a heated substrate is not surprising.

The proportions of the various forms of alumina present in a coating also depend upon the spraying conditions. Sokolova *et al.* [9] concluded that γ-Al_2O_3 tended to be formed in plasma-sprayed coatings with large substrate torch distances, low currents and high plasma gas pressures and that as the distance and pressure were reduced and current increased, δ-Al_2O_3 and an increased proportion of α-Al_2O_3 were formed. They attributed these changes to effects of substrate heating but also suggested that there were two sources of α-Al_2O_3 in the coating: unmelted α-Al_2O_3 feed particles, which tended to increase with lower input power, and secondary α-Al_2O_3 formed as a result of substrate heating. On the other hand, Zoltowski [10] concluded, from microscopic examination of plasma-sprayed coatings, that the presence of α-Al_2O_3 was entirely due to the incorporation of unmelted feed particles.

2. Metastable aluminas

There has been some confusion in the literature concerning the nomenclature for metastable forms of Al_2O_3 and their crystal structures have not been well defined because of the lack of single crystals suitable for X-ray diffraction studies [11]. The term γ-Al_2O_3 has been used both as a general description of all metastable forms based on a more or less distorted cubic close-packing (c c p) of oxygen ions [12] and for particular phases with a spinel structure. Spinel ($MgO{\cdot}Al_2O_3$) has a structure in which eight Mg ions occupy tetrahedral sites and sixteen Al ions occupy octahedral sites within a unit cell containing 32 c c p oxygen ions. To maintain charge balance in Al_2O_3 with the spinel structure, $21\frac{1}{3}$ Al ions and $2\frac{2}{3}$ cationic vacancies must be distributed over the available sites. Most studies of metastable aluminas have been concerned with products of calcination of hydroxides and these have shown that several structures with well defined X-ray diffraction powder patterns occur in sequences leading finally to α-Al_2O_3, the only stable form, in which aluminium ions are located in octahedral sites within a hexagonal close-packed (h c p) arrangement of the oxygen ions.

Two sequences of metastable forms related to spinel are observed on heating boehmite (AlOOH) and bayerite ($Al(OH)_3$). Using the generally accepted nomenclature based on X-ray powder diffraction patterns [13], these forms are:

$$\text{Boehmite} \xrightarrow{450^\circ C} \gamma\text{-}Al_2O_3 \xrightarrow{750^\circ C} \delta\text{-}Al_2O_3 \xrightarrow{1000^\circ C} \theta\text{-}Al_2O_3 \xrightarrow{1200^\circ C} \alpha\text{-}Al_2O_3$$

$$\text{Bayerite} \xrightarrow{230^\circ C} \eta\text{-}Al_2O_3 \xrightarrow{850^\circ C} \theta\text{-}Al_2O_3 \xrightarrow{1200^\circ C} \alpha\text{-}Al_2O_3$$

Both δ-Al_2O_3 and θ-Al_2O_3 give X-ray patterns with a large number of sharp lines whereas η-Al_2O_3 and γ-Al_2O_3 show a small number of broad lines which correspond with the spinel structure. A feature of the diffraction patterns for all of these metastable phases is that they show strong lines associated with nearly cubic close-packed oxygen ions (the 400 and 440 spinel-lines) which led Ervin [14] to speculate that the various forms were related to cation order–disorder phenomena within the oxygen framework.

The main difference between the X-ray powder diffraction patterns of γ-Al_2O_3 and η-Al_2O_3 is that for the γ-form the (400) and (440) lines are split and for the η-form they are not [13]. Lejus [15], however, has noted that although γ-Al_2O_3 formed during the early stages of boehmite decomposition showed splitting of these lines, further heating to 700° C resulted in the formation of a cubic structure. She suggested that this effect was associated with retention of some OH at low temperatures, a view which is supported by the observations that the water content of η-Al_2O_3 can be accounted for by surface OH but that additional water is present in γ-Al_2O_3 [16] and that only cubic γ-Al_2O_3 is observed during the crystallization of anhydrous amorphous Al_2O_3 films [17].

Electron diffraction patterns of η-Al_2O_3 and tetragonal γ-Al_2O_3 derived from bayerite and boehmite revealed diffraction spots in addition

to those expected for the spinel structure, together with continuous streaks in the case of η-Al_2O_3 [13]. These results are interpreted as arising from stacking faults on the (111) spinel planes of η-Al_2O_3 and from the order of cations and vacancies over the available sites for γ-Al_2O_3. The observation of streaking in the electron diffraction pattern of γ-Al_2O_3 prepared by oxidation of aluminium has also been attributed to stacking faults at which the cationic vacancies were located [18]. These studies suggest that η-Al_2O_3 and γ-Al_2O_3 are closely related to the spinel form and that the differences observed arise from the detailed arrangement of the cations and cationic vacancies; the precise way in which they are arranged, however, remains a matter of controversy. The phase giving an X-ray powder diffraction pattern consistent with the cubic spinel structure is generally referred to as γ-Al_2O_3 in the spray coating literature although it would be regarded as η-Al_2O_3 in the literature concerned with the products of calcination of hydroxides. To retain consistency with the spray coating usage this phase will be referred to as γ-Al_2O_3 in further discussion.

Heating γ-Al_2O_3 derived from boehmite to temperatures above about 850° C results in transformation to δ-Al_2O_3, a structure with a well-defined X-ray diffraction pattern in which the (400) and (440) spinel lines become clearly doubled and a large number of additional lines appear. A similar powder diffraction pattern has been observed in the Al_2O_3 rich region of the systems Al_2O_3–AlN, Al_2O_3–MgO and Al_2O_3–NiO [15]. X-ray powder diffraction pattern data have been indexed on the basis of a spinel superlattice structure using a tetragonal unit cell with c-axis $\frac{3}{2}$ that of spinel [19]. Electron diffraction studies of δ-Al_2O_3 prepared from boehmite showed a large number of superlattice reflections suggesting a structure based on an ordering of the cations and vacancies in a slightly distorted spinel structure. The results were consistent with a super-cell consisting of three spinel blocks stacked on each other.

Studies of the structure of single crystals of δ-(Al_2O_3–AlN) in the composition range 90 to 97 mol% Al_2O_3 suggest that it has a one dimensional periodic antiphase structure based on spinel with the cationic vacancies located in the vicinity of the antiphase boundaries [20]. The structure of δ-Al_2O_3 is probably similar but with a different modulation period.

θ-alumina is observed as a minor phase during the transformation of δ-Al_2O_3 derived from boehmite to α-Al_2O_3 and the major intermediate phase during transformation of η-Al_2O_3 derived from bayerite to α-Al_2O_3. Material with a sharp X-ray powder diffraction pattern may be prepared by hydrothermal treatment of η-Al_2O_3 [21] or by the condensation of Al_2O_3 containing about 15 wt% Cr_2O_3 from a high frequency plasma [22]. θ-Al_2O_3 is isostructural with β-Ga_2O_3 and consists of a slightly distorted cubic close-packing of oxygen ions with double edge-shared strings of octahedral co-ordinated aluminium ions joined together with corner-sharing tetrahedra. Equal numbers of octahedral and tetrahedral sites are occupied in the unit cell [23]. Thus, although the basic cubic close-packing of the anions of spinel is retained in θ-Al_2O_3, the occupation of cationic sites is quite different from that of either η-Al_2O_3, γ-Al_2O_3, or δ-Al_2O_3.

3. Formation of metastable alumina from the melt

The formation of metastable forms of alumina by flame- or plasma-spraying onto substrates, in particles condensed from the vapour which have passed through the liquid phase and in rapidly cooled melts, suggest that they are formed as a result of a quenching effect. This is the view generally adopted in the literature with little consideration being given to the reason why. Plummer [24] suggested that metastable phases were formed because the assumed tetrahedral co-ordination of Al in the liquid state was retained by rapid cooling to give cubic close-packed oxygen structures. However there are a number of objections to this explanation:

(1) As shown above, most of the Al ions are in octahedral co-ordination in γ-Al_2O_3 and δ-Al_2O_3;

(2) Recent studies of the structure of liquid Al_2O_3 suggest that Al ions are in octahedral co-ordination in the liquid [25];

(3) The very short time constant for cation rearrangement in the liquid state makes it unlikely that the liquid structure could be quenched-in at practical cooling rates.

An alternative explanation is based on nucleation kinetics and suggests that γ-Al_2O_3 has a lower energy barrier to nucleation from the liquid than α-Al_2O_3 because of a lower liquid–solid interfacial energy [26]. This means that γ-Al_2O_3 nucleates from the liquid if undercooled suf-

ficiently. It should be noted that since γ-Al_2O_3 is metastable with respect to α-Al_2O_3, its equilibrium melting point will be lower (approximately 40° C [27]) so that it cannot nucleate close to the equilibrium melting point of α-Al_2O_3. Furthermore, nucleation of γ-Al_2O_3 will only become possible at a considerable undercooling because of the relative change of the free energy differences between γ-Al_2O_3, α-Al_2O_3 and liquid with temperature. The temperature below which γ-Al_2O_3 would be expected to nucleate in preference to α-Al_2O_3 has been estimated to be approximately 1750° C [27], however, there is considerable uncertainty in the value because of the neccessity to estimate the interfacial energies between the two crystalline forms of alumina and the liquid. If γ-Al_2O_3 is nucleated, the phase finally observed will depend upon the subsequent thermal history of the solid phase and the kinetics of transformation of γ-Al_2O_3 to δ-Al_2O_3, θ-Al_2O_3 and α-Al_2O_3. This hypothesis provides an explanation for the observation that spheroidized particles consist of γ-Al_2O_3 or δ-Al_2O_3 at particle sizes less than about 15 μm, but α-Al_2O_3 at larger sizes and also suggests that γ-Al_2O_3 is nucleated in plasma- and flame-sprayed coatings for similar reasons. Under spheroidization conditions, in which droplets cool in isolation, homogeneous nucleation occurs at large undercoolings, $\Delta T = 0.2\,T_m$, where T_m is the absolute melting point [26]. The undercooling would be expected to be lower droplets solidifying in contact with a substrate because of heterogeneous nucleation and therefore the degree of undercooling would be expected to depend upon both the cooling rate and the particle dimensions. Some measurements of the undercooling of splat-quenched metals have been carried out under conditions of cooling rate and particle size comparable with those for plasma- and flame-coating which suggests that the undercooling approaches the value of $0.2\,T_m$ observed for homogeneous nucleation [28, 29]. The formation of γ-Al_2O_3 in coatings can thus be explained on the basis of nucleation kinetics provided that the liquid cooling rate is sufficiently high. It is possible however that the undercooling could differ from particle to particle, depending upon the liquid cooling rate and, since this would in turn depend upon the size, velocity and temperature of individual particles in the spray stream, it is possible that α-Al_2O_3 is directly nucleated in some particles.

An alternative explanation for the origin of α-Al_2O_3 in coatings is that, since the initial feed material is usually α-Al_2O_3, any particles which did not melt completely would contain a pre-existing α-Al_2O_3 nucleus and they would therefore crystallize to this form. Even a microscopic unmelted particle within a molten droplet would act in this way. The incorporation of completely unmelted particles within the coating would be a rare occurrence because the rate of spreading and solidification of droplets on the substrate is so rapid that the spray particles effectively strike a completely solid surface and unmelted particles would bounce off.

The phase finally observed at ambient temperatures will also depend upon the cooling rate of any γ-Al_2O_3 formed since it transforms rapidly above 1200° C to δ-Al_2O_3, θ-Al_2O_3 or α-Al_2O_3. The effect of substrate temperature would be particularly important in this respect providing an explanation for the observations that γ-Al_2O_3 is the predominant phase with a cold substrate whereas δ-Al_2O_3 predominates for a substrate temperature of 900° C and α-Al_2O_3 above 1100° C [5].

4. Particle impact with the substrate

The crystal structure of plasma- and flame-sprayed coatings clearly depends upon the conditions under which the liquid droplets spread and solidify on impact with the substrate and their subsequent thermal history. When a molten droplet strikes the substrate it will flatten to form a disc and the rate of heat transfer to the substrate by conduction will rapidly increase as the area of contact increases. A simple analysis by Jones [30] of the splat-quenching of metals suggested that the freezing velocity was orders of magnitude lower than the rate of flattening so that the two processes could be treated as separate events. A model based on the flattening of a cylinder between parallel plates gave the following relationship for the thickness of the disc, S,

$$S = \left(\frac{2\eta d^3}{33\rho v}\right)^{0.25}, \qquad (1)$$

where η is the liquid viscosity, d is the drop diameter, v is the drop velocity, and ρ is the liquid density.

Application of this equation to aluminium, however, gave values for S of about one-fifth those observed experimentally, suggesting that

the assumption of the independence of flattening and freezing was not correct. In fact Jones used freezing velocities determined by heat flow considerations whereas the liquid undercools considerably in splat-quenching and the freezing velocity would be expected to approach the very much higher intrinsic value observed in highly undercooled melts.

A more elaborate treatment of the impact of molten droplets against a cold substrate has been given by Madejski [31] who attempted to include viscous flow, surface tension and crystallization kinetics. Simplifying Madejski's treatment by assuming that flattening is complete before crystallization becomse significant, gives, for the ratio of the diameter of flattened disc, D, to the drop diameter, d, $\xi = D/d$,

$$\frac{3\xi^2}{W} + \frac{1}{R}\left(\frac{\xi}{1.29}\right)^5 = 1, \quad (2)$$

which applies for value of the Weber number, W and the Reynolds number, R, greater than 100 where,

$$W = \frac{\rho\, d v^2}{\sigma}, \quad (3)$$

$$R = \frac{\rho\, d v}{\eta} \quad (4)$$

and where σ is the liquid surface tension. Using the appropriate values for σ and ρ for liquid Al_2O_3 at its melting point (0.68 Nm^{-1} and 3.05 gm cm^{-3} [32]) gives a value of W in the range 1000 to 20000 for plasma spraying conditions of d equal to 20 to 100 μm and v equal to 100 to 400 m sec^{-1}. For realistic values of ξ, the factor $3\xi^2/W$ is negligible and may be neglected (surface tension effects only become significant for particle sizes less than about 10 μm). This simplification gives:

$$\xi = 1.29\left(\frac{\rho\, d v}{\eta}\right)^{0.2}, \quad (5)$$

for $R < 100$ and $\xi = 1.29\,((\rho\, d v/\eta) + 0.95)^{0.2}$.

Measurements of the temperatures of Al_2O_3 particles in a plasma-spray stream have shown that most particles have a temperature near the melting point because of the thermal inertia resulting from the need to supply the heat of fusion. The maximum temperature reached by a significant proportion of the particles is probably 2500° C [33]. The minimum temperature of a liquid droplet will not be the equilibrium melting point but the temperature of undercooling for homogeneous nucleation ($\simeq 0.8\,T_m$) which is about 1600° C for Al_2O_3. The viscosity range of liquid droplets, determined from the data of Elyutin *et al.* [34], therefore varies from 0.15 poise (at 2500° C) to 5 poise (at 1600° C) with a most probable value of 0.5 poise for particles close to the melting point. Since the particles must first melt completely before undercooling to the maximum extent, the proportion of particles with viscosities greater than 0.5 poise would be expected to increase with distance from the injection point. A study in which ξ was measured for Al_2O_3 particles with a narrow size distribution and mean velocity of 300 m sec^{-1} gave values of 2.8 to 3.5 which are in excellent agreement with calculated values for particles with temperatures near the melting point [33]. The lamellar thickness for Al_2O_3 particles, 50 μm in diameter, as a function of temperature and velocity calculated using Equation 5 is shown in Fig. 1, assuming that the lamellae are of uniform thickness. Reported values of lamellar thicknesses for plasma-sprayed Al_2O_3 powders lie in the range between 2 and 4 μm [10] in reasonable agreement with the above calculations for particles near the melting point and recognizing that the lamellae are not of uniform thickness. The assumption that flattening and solidification are separate events is therefore probably satisfactory for lamellae thicknesses of a few micrometres but a limiting thickness, pro-

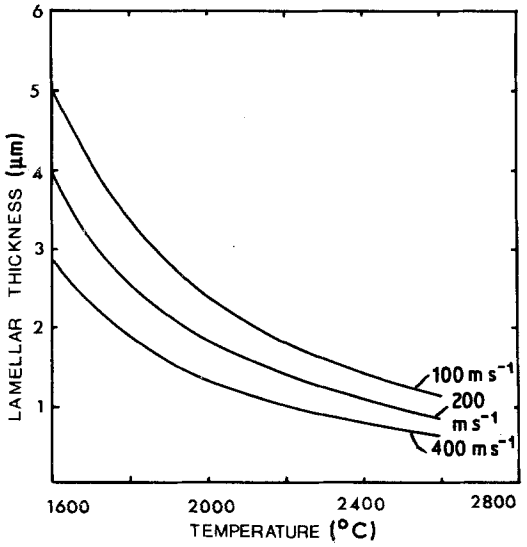

Figure 1 Lamellar thickness for 50 μm Al_2O_3 particles as a function of initial temperature and velocity, estimated from Equation 5.

bably of about 1 μm must be reached at which the thickness is controlled by the solidification kinetics.

5. Solidification

The cooling rate of splat-quenched materials has been the subject of many studies using both direct measurement and indirect estimation based on dendrite arm spacing. These have shown that the cooling rate values for the "gun technique", in which a liquid droplet is projected at high velocity against a cold substrate, lies in the range 10^6 to 10^8 K sec^{-1} [35]. Heat transfer calculations have shown [36] that, at small lamellae thicknesses, the cooling rate of the solid is determined by the nature of the interface between the lamella and the substrate and is independent of the thermal conductivity of the substrate. Comparison between calculated and experimental data for splat-cooled metals suggest that the value of the heat transfer coefficient at the interface is of the order of 10^5 W m^{-2} K^{-1} [35].

The evidence suggests that the flattened disc undercools to an extent comparable with that observed in isolated droplets [28, 29] and nucleated crystals therefore grow rapidly into the liquid at the limiting growth rate. Liberation of the heat of fusion would result in an increase in temperature of the liquid, thus suppressing further nucleation and the temperature would increase towards the equilibrium melting point at a rate determined by the crystal growth rate and the rate of heat transfer to the substrate. If the temperature of the particle reached the equilibrium melting point, the rate of solidification would be controlled thereafter by the rate of heat removal; both of these situations would tend to result in a columnar microstructure.

If the rate of heat transfer to the substrate was such that the liquid temperature continued to decrease after initial nucleation the nucleation rate would be expected to increase because of its extreme sensitivity to undercooling. The rate of solidification would, in this case, tend to be controlled by the rate of nucleation, resulting in a very fine, equiaxed microstructure. The columnar microstructure revealed on the fracture surfaces of plasma-sprayed alumina [37] suggests that the rate of heat removal is comparable to, or less than, the rate of heat generation.

6. Thermal history of flattened droplets

Calculation of the thermal history of a flattened droplet is limited by the uncertainty in the values of crystal growth rate, degree of undercooling and interfacial heat transfer coefficient. Using the "most probable" values for crystal growth rate of 10 cm sec^{-1} [26] heat transfer coefficient, h, of 10^5 W m^{-2} K^{-1} and nucleation temperature of 1700° C, together with published values for the heat capacity and heat of fusion [27] gives the results shown in Fig. 2. For cold substrates, increasing the lamellae thickness has the effect of increas-

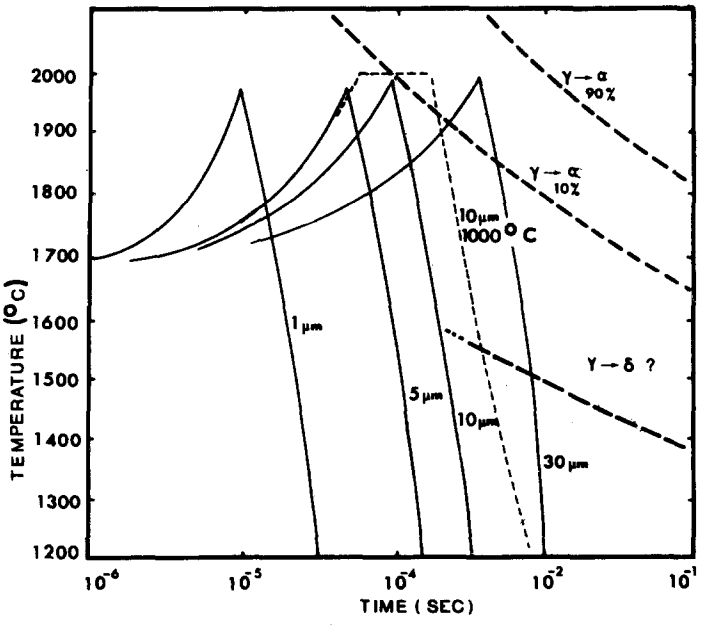

Figure 2 Estimated time–temperature relationships for Al_2O_3 lamellae on a substrate at 100° C or 1000° C as a function of thickness. Extrapolated data for the γ-Al_2O_3 to α-Al_2O_3 [39] and γ-Al_2O_3 to δ-Al_2O_3 [6] transformations are also shown.

ing the solidification time proportionately since the peak temperature does not quite reach the equilibrium melting point. At high substrate temperatures, however, the reduced heat transfer rate allows the temperature to reach the equilibrium melting point and the time for solidification is increased because it is now controlled by the heat removal rate. This is illustrated in Fig. 2 for lamellae of thickness 10 μm at substrate temperatures of 1000° C.

The cooling rate after solidification will be determined by the disc thickness, interfacial heat transfer coefficient and substrate temperature. If the Biot Number (B), for the disc, is less than 0.1, the cooling rate is controlled by the interfacial heat transfer coefficient and the thermal gradient within the disc is small [38].

$$B = \frac{hS}{k} \tag{6}$$

where k is the thermal conductivity of the disc. For Al_2O_3, this condition applied for discs less than approximately 10 μm thick if h is 10^5 W m^{-2} K^{-1}.

The cooling rate of the front and rear faces will not differ significantly for values of B of about 0.1, but the difference will increase as the disc thickness increases. The cooling curves for the 30 μm case shown in Fig. 2 are for the rear face. The cooling rate is directly proportional to the lamellar thickness up to 10 μm, and ranges from 3.5×10^7 K sec^{-1} at 1 μm to 3.5×10^6 K sec^{-1} at 10 μm, between 2000 and 1200° C for a cold substrate. The cooling rate is reduced to approximately 10^6 K sec^{-1} for a substrate at 1000° C.

7. Formation of α-Al_2O_3

The observations that the fraction of α-Al_2O_3 in coatings prepared using α-Al_2O_3 feed powders increases with both their particle size and decreasing torch power input [33] is consistent with the view that α-Al_2O_3 is formed from unmelted nuclei. Measurements of particle temperatures in spray streams have shown that the fraction of partially melted particles increases rapidly as the particle size is increased [33]. This therefore suggests that α-Al_2O_3 is formed in deposits only by nucleation from unmelted seeds and that γ-Al_2O_3 is the product of the solidification of droplets which do not contain these nuclei. According to the hypothesis previously developed for the formation of metastable phases in Al_2O_3 solidified from its melt [26], these observations suggest that most of the molten particles in the spray stream with diameters, d, in the range 10 μm $< d <$ 100 μm undercool below the temperature at which γ-Al_2O_3 is nucleated in preference to α-Al_2O_3 (estimated to be around 1750° C), i.e. an undercooling greater than approximately 0.15 T_m in agreement with the estimated undercooling during splat-quenching.

The estimated time–temperature relationship for 10% and 90% transformation of γ-Al_2O_3 to α-Al_2O_3, extrapolated from lower temperature data [39], is shown superimposed on the calculated thermal history curves for lamellae of various thicknesses in Fig. 2. This suggests that transformation to α-Al_2O_3 during crystallization would become significant at lamellae thicknesses greater than approximately 20 μm for cold substrates, and thicknesses greater than 10 μm for substrates at temperatures greater than 1000° C. An additional factor in the transformation of α-Al_2O_3 during solidification is the increased effective heat of fusion and higher equilibrium melting point for α-Al_2O_3 which would result in an acceleration of the transformation once it commenced. For the normal range of lamellae thickness in plasma- and flame-sprayed coatings using powder feed systems (with $d < 5$ μm) formation of α-Al_2O_3 during crystallization would not be expected to be significant even if the substrate was heated to several hundred degrees. This explains why it is necessary to heat the substrate to a temperature at which transformation of γ-Al_2O_3 to α-Al_2O_3 occurs during deposition (at about 1200° C) and it is necessary to heat the substrate to about 1450° C to obtain a dense Al_2O_3 coating [9]. The hypothesis outlined above provides an explanation why α-Al_2O_3 is formed to a greater extent in flame-coatings using a rod-feed sprayed onto a heated substrate [8] since, for this case [3], the lamellae thickness is greater (about 10 μm). This occurs because the end of the rod must melt before it can be detached and consequently the spray stream tends to consist of intermittent bursts of large particles [40].

The good agreement between published experimental data and the model proposed also suggests that the various assumptions concerning the degree of undercooling, the interfacial heat transfer coefficient and the limiting crystal growth rate are reasonable.

8. Formation of δ-Al_2O_3

Most studies of the structure of alumina coatings prepared by rod [3] and powder [9] flame-spraying or plasma-spraying [5, 7, 9] onto cold substrates report that the structure produced consists of a mixture of the γ-Al_2O_3 and α-Al_2O_3 forms. A predominantly δ-Al_2O_3 coating is formed only if sprayed onto a substrate heated to 900° C [5]. δ-Al_2O_3 is also observed in Al_2O_3 prepared in a high frequency plasma with a relatively slow cooling rate of 10^4 K sec^{-1} [41]. This suggests that γ-Al_2O_3 is the phase formed at large undercooling of liquid alumina, that it is retained on rapid quenching, but that slow cooling rates allow the relatively minor rearrangement of the aluminium ions to take place which results in the δ-Al_2O_3 structure [26].

Extrapolated kinetic data for the transformation of plasma sprayed γ-Al_2O_3 to δ-Al_2O_3 taken from reference [6] have also been superimposed on the time–temperature relationships for deposited Al_2O_3 in Fig. 2. Although the author pointed out that the data has limited reliability and the extrapolation is very large, it gives a qualitative comparison with the γ-Al_2O_3 to α-Al_2O_3 transformation. The transformation of γ-Al_2O_3 to δ-Al_2O_3 is quite different from the transformation to α-Al_2O_3 since it is apparently an ordering reaction whereas the latter is an irreversible transformation from a metastable to a stable phase involving complete atomic rearrangement. The γ-Al_2O_3 to δ-Al_2O_3 reaction would be expected to have an upper temperature limit above which the γ-Al_2O_3 (disordered) phase alone existed. No direct data is available for these reactions, however, since δ-Al_2O_3 is not observed in flame- and plasma-sprayed coatings onto cold substrates, but is the only phase observed in submicrometre-diameter plasma-prepared powders cooled at about 10^4 K sec^{-1}. The γ-Al_2O_3 region probably lies above 1600° C, as illustrated in Fig. 2.

This hypothesis therefore suggests that δ-Al_2O_3 observed in coatings sprayed onto initially cold substrates [6, 9] must arise from a heating of the coating during deposition.

9. Conclusions

An examination of the processes occurring during the impact and solidification of thermally sprayed alumina coatings suggests that the liquid droplets flatten completely before crystallization becomes significant and that γ-Al_2O_3 is homogeneously nucleated if the initial droplet is completely molten, because the energy barrier to nucleation of γ-Al_2O_3 is less than that of α-Al_2O_3. Particles which are not completely molten crystallize to α-Al_2O_3 from pre-existing nuclei. The thermal history of the droplets after solidification is such that if γ-Al_2O_3 is nucleated it is retained to room temperature in plasma-sprayed deposits even if the substrate is heated to about 900° C. δ-Al_2O_3 is only formed if the substrate is heated sufficiently (> 900° C) for the transformation of γ-Al_2O_3 to δ-Al_2O_3 to occur during cooling. The larger lamellar thickness in deposits flame-sprayed using the rod process modifies the thermal history after solidification so that δ-Al_2O_3 and α-Al_2O_3 are more readily formed on heated substrates.

Acknowledgements

The work described in this paper was carried out whilst the author was on leave at the Laboratoire de Thermodynamique, Université de Limoges, France and special thanks are due to Professor P. Fauchais for making this possible.

References

1. H. S. INGHAM and A. P. SHEPARD, "METCO Flame Spray Handbook" (METCO, New York, 1965).
2. N. N. AULT, *J. Amer. Ceram. Soc.* **40** (1957) 69.
3. V. S. THOMPSON and O. J. WHITTEMORE, *Bull. Amer. Ceram. Soc.* **47** (1968) 637.
4. P. ZOLTOWSKI, *Rev. Int. Hautes. Temper. et Refract.* **6** (1969) 65.
5. V. F. EICHORN, J. METZLER and W. EYSEL, *Metalloberflache* **26** (1972) 212.
6. I. R. KOZLOVA, *Izv. Akad. Nauk. S.S.S.R. Neorg. Mat.* 7 (1971) 1372.
7. D. G. MOORE, A. G. EUBANKS, H. R. THORNTON, W. D. HAYES and A. W. CRIGLER, Technical Report Number A.R.L. 59, Contract AF 33 (616)-58-19 Final Summary Report 1961.
8. J. B. HUFFADINE and A. G. THOMAS, *Powder Metall.* 7 (1964) 290.
9. T. V. SOKOLOVA, I. R. KOZOLVA, KH. DERKO and A. V. KIIKO, *Izv. Akad. Nauk. S.S.S.R. Neorg. Mat.* 9 (1973) 611.
10. P. ZOLTOWSKI, *Rev. Int. Hautes. Temper. et Refract.* **5** (1968) 253.
11. K. WEFARS and G. M. BELL, Technical Paper No. 19, Alcoa Research Laboratories, 1972.
12. A. F. WELLS, "Structural Inorganic Chemistry" (Clarendon Press, Oxford, 1962) p. 560.
13. B. C. LIPPENS and J. H. DE BOER, *Acta. Cryst.* **17** (1964) 1312.
14. G. ERVIN, *ibid.* **5** (1952) 103.
15. A. M. LEJUS, *Rev. Int. Hautes. Temper. et Refract.* **1** (1964) 53.

16. D. S. MacIVER, H. H. TOBIN and R. T. BATH, *J Catalysis* **2** (1963) 485.
17. A. L. DRAGOO and J. J. DIAMOND, *J. Amer. Ceram. Soc.* **50** (1967) 568.
18. J. M. COWLEY, *Acta Cryst.* **6** (1953) 53.
19. H. P. ROOKSBY and C. J. M. ROOYMANS, *Clay Minerals Bull.* **4** (1961) 234.
20. A. LEFEBVRE, *J. Appl. Cryst.* **8** (1975) 235.
21. G. YAMAGUCHI, I. YASUI and W. CHUI, *Bull. Chem. Soc. Japan* **43** (1970) 2487.
22. R. McPHERSON, *J. Mater. Sci.* **8** (1973) 859.
23. S. GELLER, *J. Chem. Phys.* **33** (1960) 626.
24. M. PLUMMER, *J. Appl. Chem.* **8** (1958) 35.
25. A. NUKUI, H. TAGAI, H. MORIKAWA and S. I. IWAI, *J. Amer. Ceram. Soc.* **59** (1976) 534.
26. R. McPHERSON, *J. Mater. Sci.* **8** (1973) 851.
27. M. W. CHASE, J. L. CURNUTT, R. A. McDONALD and A. N. SYVERUD, *J. Phys. Chem. Ref. Data* **7** (1978) 793.
28. K. LOHBERG and H. MULLER, *Z. Mettalkunde* **60** (1969) 231.
29. I. S. MIROSHNICHENKO and V. A. ZAKHAROV, *Ind. Lab.* **39** (1969) 362.
30. H. JONES, *J. Phys. D* **4** (1971) 1657.
31. J. MADEJSKI, *Int. J. Heat Mass Transfer* **19** (1976) 1009.
32. B. S. MINTIN and YU. A. NAGIBIN, *Zh. Fiz. Khim.* **44** (1970) 1325.
33. A. VARDELLE, M. VARDELLE, R. McPHERSON and P. FAUCHAIS, Proceedings of the Ninth International Thermal Spraying Conference, Amsterdam, May 1980 (Netherlands Institute of Lastechniek, The Hague, 1980) p. 155.
34. V. P. ELYUTIN, V. I. KOSTIKOV, B. S. MINTON and YU. A. NAGIBIN, *Russ. J. Chem.* **43** (1969) 316.
35. H. JONES, *Rep. Prog. Phys.* **36** (1973) 1425.
36. R. C. RUHL, *Mater. Sci. Eng.* **1** (1967) 313.
37. V. WILMS and H. HERMAN, *Thin Solid Films* **39** (1976) 251.
38. F. KREITH, "Principles of Heat Transfer" (Intext Educational Publishers, New York, 1973) p. 140.
39. C. J. P. STEINER, D. P. H. HASSELMAN and R. M. SPRIGGS, *J. Amer. Ceram. Soc.* **54** (1972) 412.
40. R. LINGUET, G. RODIER and J. ROGERS, *Bull. Soc. Fr. Ceram.* **54** (1961) 39.
41. M. S. J. GANI and R. McPHERSON, *J. Aust. Ceram. Soc.* **8** (1972) 65.

Received 28 February and accepted 5 June 1980.